Generation of orbital angular momentum and focused beams with tri-layer medium metamaterial*

Zhi-Chao Sun(孙志超), Meng-Yao Yan(闫梦瑶), and Bi-Jun Xu(徐弼军)†

School of Sciences, Zhejiang University of Science and Technology, Hangzhou 310023, *China*

(Received 10 May 2020; revised manuscript received 8 June 2020; accepted manuscript online 1 August 2020)

We propose a metal/dielectric tri-layer metamaterial for wavefront shaping. By arranging the element in an array with a constant phase gradient and irradiated it with a plane wave, focused and focused vortex beams can be obtained. The designed metamaterial features the excellent capability of focused/focused vortex beams generation within the operating frequency range of 30 GHz–34 GHz. The simulation results are consistent with the theoretical analyses.

Keywords: metamaterial, phase shift, wave-front shaping, orbital angular momentum

PACS: 41.20.Jb, 42.25.Bs, 92.60.Ta **DOI:** 10.1088/1674-1056/abab79

1. Introduction

Metamaterial, a kind of synthetic material, has material properties including negative refraction, electromagnetic cloaking which are not available in natural materials.[1,2] Dielectric/metal metamaterials allows tailored electromagnetic properties flexibly and effectively such as amplitude and phase by controlling the size, shape, and relative arrangement of it.[3–5] Few-layered metamaterials have shown excellent electromagnetic properties for wavefront shaping.

Firstly, we designed an array for generating a focused vortex beam[6,7] carrying orbital angular momentum (OAM). The orbital angular momentum carried is one of the fundamental physical properties of electromagnetic waves.[8] With various orthogonal OAM modes, vortex beams can greatly increase the information capacity.[9] Therefore, vortex beams have recently been considered for high-capacity communications.[10,11]

There are several conventional methods of generating vortex waves, such as spiral phase plate, antenna arrays,[12,13] holographic diffraction gratings,[14] circular traveling-wave antenna,[15–17] circular polarized patch,[18] dielectric resonate antenna, [19–22] and multi-arm spiral patch.[23] However, these systems are bulky and could not be integrated.[24,25] Therefore, optical metamaterials have attracted progressively increasing attention because of the advantages of compactness, unprecedented ability to modulate electromagnetic waves, and low cost.[26]

In addition, we have fabricated a tri-layered metamaterial to generate a focused beam. In recent years, reflectors and lens antenna focusing are the main means of electromagnetic focusing. However, both of them have advantages and disadvantages.[27,28] The focal spot of the reflector focusing antenna is tiny, but its working efficiency is low due to the feed shielding and is generally bulky.[29,30] Although the lens focusing antenna has no feed shielding loss, its protruding lens structure is not suitable for some flat antenna. In conclusion, designing a low-profile, high-density, and small-volume metamaterial plays a significant role in accelerating the development of nanophotonics technology.[31–36]

In this paper, we have designed a metamaterial element that covers the full phase range by adjusting the parameters. We achieved effective simulation results by making use of a few unit cells. Our focusing metamaterial exhibits a measured gain of 25 dBi and focused vortex array achieved a working efficient of 85% at the central operating frequency of 32 GHz. The simulation results show consistency with the analysis and reach the design expectation.

2. Geometries of unit and metamaterial design

In our case, we use three layers of aluminum (Al) and two dielectric substrates for the design of the metamaterial element. During early design phase, we have considered other structures, such as single layer and other multi-layer. However, after simulated, we found that the single-layer metasurface cannot cover 2π phase in the frequency we designed, and other multi-layer metamaterials' transmission efficiency is low. Finally, we adopted the three-layers metamaterial. Concerning Fig. 1, the period length of the unit cell is $p = 3$ mm. The thickness d_1 of each Al layer is 0.035 mm and perforated with two arrays of coaxial annular apertures (CAAs). The dielectric layer has a thickness of $d_2 = 0.8$ mm and a permittivity of 2.0. After repeated simulations, the outer radius of the outer ring and the inner radius of the inner ring are respectively fixed at 1.5 mm and 0.1 mm. Then we adjusted the inner radius a of the outer ring to obtain the full range of phases. The outer radius b is one half of a. The plane waves are propagating along

*Project supported by the Natural Science Foundation of Zhejiang Province, China (Grant No. LY20F050001).

†Corresponding author. E-mail: xubijun@zust.edu.cn

+z direction, by tuning the radius of CAAs, the transmitted waves are refracted in the prescribed direction to generate focused or OAM beams.

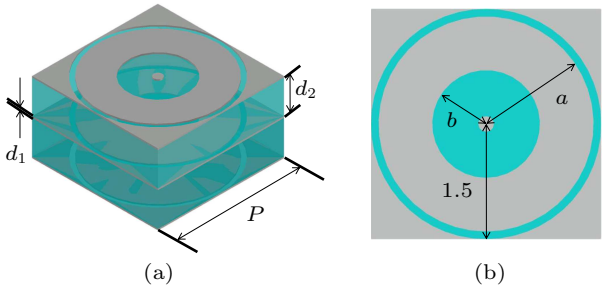

Fig. 1. (a) Scheme of the unit used in the design, (b) top view of the unit.

Table 1. The radius a corresponding to the phase and transmission amplitude of our designed model.

a/mm	Transmission phase/(°)	Theoretical transmission phase/(°)	Amplitude
1.4	–156.0	–157	0.73
1.347	–110.0	–112	0.75
1.121	–66.2	–67	0.79
0.997	–21.5	–22	0.82
0.924	22	23	0.86
0.868	68.3	68	0.88
0.794	112	113	0.92
0.732	156	158	0.93

We start by investigating the transmission of the prototype of a tri-layered metamaterial concerning the different inner radii of CAAs. As shown in Table 1 and Fig. 2, when a ranges from 0.732 mm to 1.4 mm, the phase decreases smoothly from 158° to −157°. As an efficient resonant unit, it provides full control of the phase of the transmitted wave without sacrificing the transmittance.

Arbitrary phase distribution can be obtained by reasonably arranging the unit cells with different radius. To obtain the focused or OAM beams, eight phases with 45° difference are selected to form the metamaterial array. Here are the values of a corresponding 8 phases and transmission amplitudes at 32 GHz.

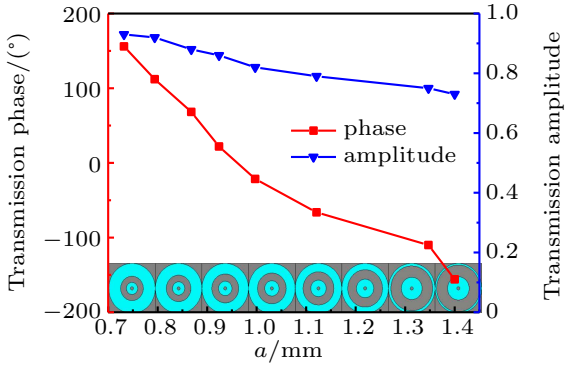

Fig. 2. The radius a corresponding to the phase shift and transmission amplitude at 32 GHz.

In this paper, eight CAAs with different radii are selected to form the focused metamaterial. The radius a decreases from inside out from 1.4 mm in region one to 0.732 mm in region eight, corresponding to the phase increases from −157° to 158°. Then for the focused vortex metamaterial, the array is also split into eight regions. The phase linearly increases from −157° in region one to 158° in region eight clockwise with a fixed increment of 45°. The schematic diagram of the metamaterials are shown in Fig. 3.

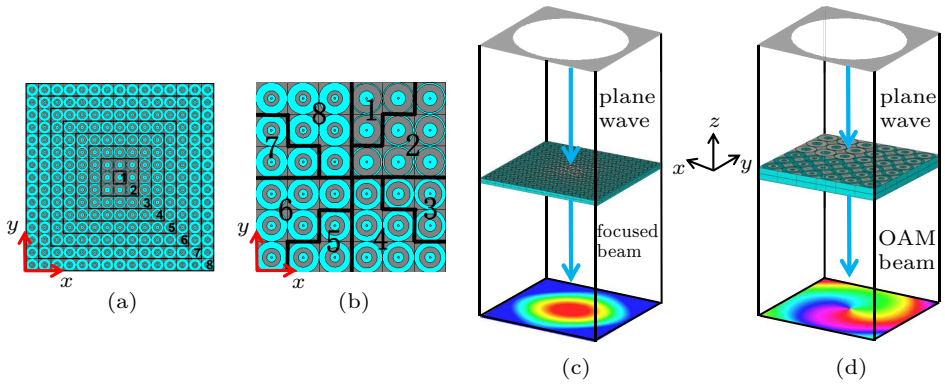

Fig. 3. Panels (a) and (b) are the planes of focused and focused vortex metamaterial, panels (c) and (d) are the three-dimensional (3D) view of metamaterial arrays.

3. Simulation and analysis

The theoretical predictions stated above are verified by CST simulations. We characterize the near-field and far-field EM performances of metadevices. The designed focused metamaterial is excited by a plane wave in the x–y plane. Firstly, we characterize the focused metamaterials' property.

Referring to the simulated electric and far-field distribution as shown in Fig. 4, we can clearly see the focused metamaterial perfectly focused the beam at the focal point which are about 15 mm away from the metamaterial with a high gain. The results show that the focused wave can be generated effectively from 30 GHz to 34 GHz, which works best at 32 GHz. We also

plot two-dimensional (2D) gain patterns at different frequencies for the sake of clarity to show the performance of the focused metamaterial. As shown in Fig. 5, the device achieved a total gain of about 25 dBi from 30 GHz to 34 GHz. Moreover, the side lobe is small indicating good collimation of the radiative power along the z axis from the feed source and the far-field results further verify the characteristic of the focused metamaterial.

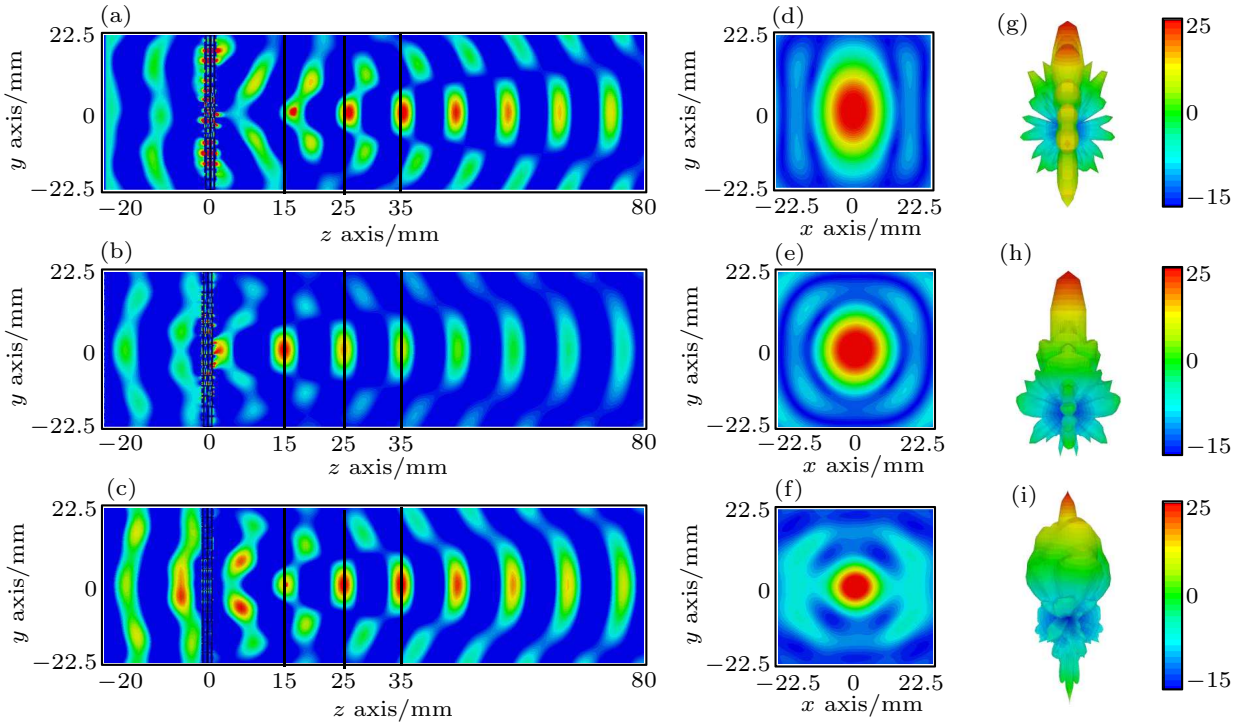

Fig. 4. (a)–(c) Focused electric field distribution of the y–z plane at 30, 32, and 34 GHz. (d)–(f) Focused electric field distribution of the x–y plane at 30, 32, and 34 GHz. (g)–(i) Focused far-field pattern of the metamaterial at 30 GHz, 32 GHz, and 34 GHz.

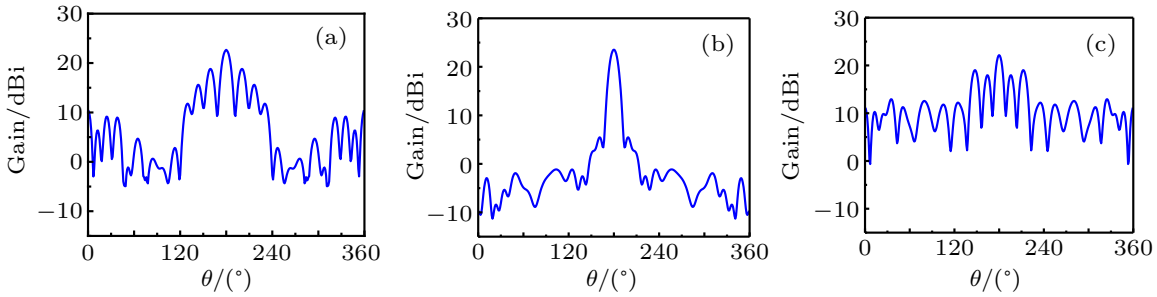

Fig. 5. (a)–(c) Simulation gains at 30 GHz, 32 GHz, and 34 GHz.

Secondly, we calculated the radiation performances of OAM focused vortex beam. The generation of OAM beam requires to combine the initial phase and the spiral phase. For position $A\ (x,y)$ on the array, the initial phase φ_1 which radiated by feed source can be calculated as

$$\varphi_1 = \frac{2\pi}{\lambda}\left(\sqrt{x^2+y^2+d^2}-d\right)+\varphi_0 \tag{1}$$

with d being the focal length, φ_0 being the reference phase, and λ is the wavelength of our design frequency. Here we set $\varphi_0 = 0^\circ$ and $d = 15$ mm. The second part of the calculation is in order to make the beam carry the spiral phase, and it can be expressed by the following formula:

$$\varphi_2 = l \cdot \arctan\left(\frac{x}{y}\right), \tag{2}$$

where l is the mode number of topological charge and we choose $l = 1$. Thus, the total phase distribution transmitted by metamaterial can be simplified to

$$\varphi_{\mathrm{OAM}} = \varphi_1 + \varphi_2. \tag{3}$$

Then, the phase distributions for $l = 1$ are shown in Figs. 6(a)–6(c).

After simulating calculation, we simulated its far-field property by CST. In general, the far-field refers to the spatial range with the feed source as the center and the radius beyond three times of the wavelength. In this paper, the wavelength ranges from 8 mm to 10 mm. We used linearly polarized plane waves as the feed source. Referring to the electric field energy distributions and phase profiles (35 mm behind the metamaterial) which recorded by a field monitor at x–y plane as shown

in Figs. 6(d)–6(i), our simulation intuitively displays the unprecedented performance of the metamaterial.

As expected in the operating frequency, the amplitude intensity of focused vortex beams at the centre is the minimum, due to the vector singularity, thus showing their capability of converting plane waves into focused vortex beams. Based on the simulation results, we can calculate the working efficiency of the focused vortex beam which is defined as the ratio of the power within the focused vortex beam to that of the incident wave. Therefore, the numerical efficiencies we measured are more than 85% for all the frequencies varied from 30 GHz to 34 GHz. This lays a foundation for the further study of the wireless communication system. In this paper, we only take the mode number $l = 1$ as an example to illustrate the efficiency and feasibility of the metamaterial.

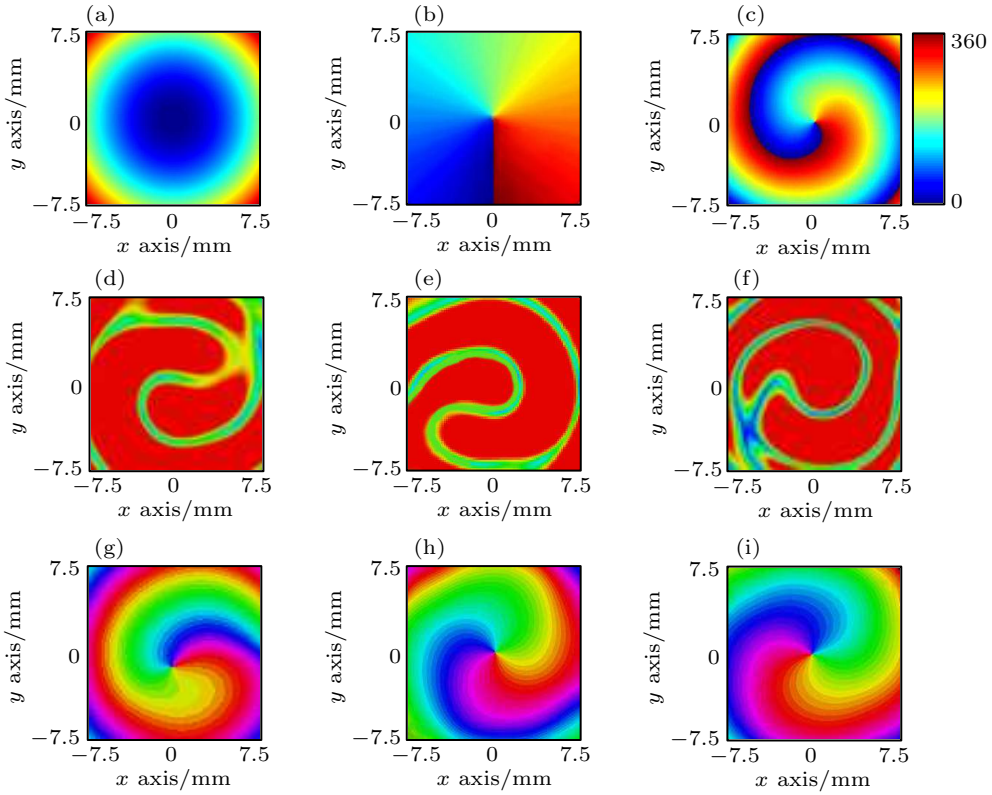

Fig. 6. (a) Incident initial phase; (b) spiral phase; (c) total phase; (d)–(f) Focused vortex electric field distribution at 30, 32 and 34 GHz; (g)–(i) Simulation results of focused vortex phase at 30 GHz, 32 GHz, and 34 GHz.

4. Conclusion

In conclusion, we arranged the metamaterial unit cells in concentric circles or distributed in 8 quadrants by gradient, and proposed a simple design which is based on the metamaterial to generate focused beam and focused vortex wave at 30 GHz–34 GHz. We improve the working efficiency by deliberately selecting the geometric parameters of the unit cell, the locations of CAAs at different layers, and the arrangement of the phase gradient. The simulation results agree well with the theoretical prediction. The designed metamaterials sample exhibits excellent capabilities of focused and focused vortex beams generation. To sum up, the proposed metamaterials provide a new method in the application of communication systems.

References

[1] Xiao H D, Sun H Y, Gu C Q, Li Z, Chen X L and Xu B J 2019 *Prog. Electron. Res.* **80** 111
[2] Fan B, Ba Z L and Xiong W 2018 *Opt. Express* **26** 25693
[3] Zhang Y, Yang L, Wang H, Zhang X and Jin X 2018 *IEEE Antenn. Propag. Lett.* **17** 172
[4] Xu H X, Liu H, Ling X, Sun Y and Yuan F 2017 *IEEE T. Antenn. Propag.* **65** 7378
[5] Yu S, Li L, Shi G, Zhu C, Zhou X and Shi Y 2016 *Appl. Phys. Lett.* **108** 121903
[6] Fei D, Chen Y T and Bozhevolnyi S I 2020 *Nanophotonics* **9** 371
[7] Mehmood M Q, Mei S T, Hussain S, Huang K, Siew S Y, Zhang L, Zhang T H, Ling X H, Liu H, Teng J H, Danner A, Zhang S and Qiu C W 2016 *Adv. Mater.* **28** 2533
[8] Li T J, Liang J G, Li H P and Liu Y Q 2016 *Chin. Phys. B* **25** 094101
[9] H ou H S, Wang G M, Li H P, Guo W L, Li T J and Cai T 2017 *Chin. Phys. B* **26** 057701
[10] Wei Z Y, Cao Y, Su X P, Gong Z J, Long Y and Li H Q 2013 *Opt. Express* **21** 10739
[11] Zhang D, Cao X Y, Yang H H, Gao J and Lv S Q 2019 *Chin. Phys. B* **28** 034204
[12] Pendry J B, Schurig D and Smith D R 2006 *Science* **312** 1780
[13] Zhao Y, Belkin M A and Alù A 2012 *Nat. Commun.* **3** 870
[14] Wei Z Y, Cao Y, Fan Y C, Yu X and Li H Q 2011 *Opt. Express* **19** 21425
[15] Odit M, Kapitanova P, Belov P, Alaee R, Rockstuhl C and Kivshar Y S 2016 *Appl. Phys. Lett.* **108** 221903
[16] Lin B Q, Guo J X, Huang B G, Fang L B, Chu P and Liu X W 2018 *Chin. Phys. B* **27** 054204

[17] Zheng W, Zheng S, Hui X, Chen Y, Jin X, Chi H and Zhang X 2017 *IEEE Antenn. Propag. Lett.* **16** 194
[18] Jiang Z H, Kang L, Hong W and Werner D H 2018 *Phys. Rev. Appl.* **9** 064009
[19] Guo Z and Yang G 2017 *IEEE Antenn. Propag. Lett.* **16** 404
[20] Yu S, Li L, Shi G, Zhu C and Shi Y 2016 *Appl. Phys. Lett.* **108** 241901
[21] Cvijetic N, Milione G, Ip E and Wang T 2015 *Sci. Rep.* **5** 15422
[22] Zhao M M, Fu S F, Zhou S, Song Y L, Zhang Q, Yin Y Q, Zhao Y T, Liang H and Wang X Z 2020 *Chin. Phys. B* **29** 054210
[23] Liu K, Cheng Y, Yang Z, Wang H, Qin Y and Li X 2015 *IEEE Antenn. Propag. Lett.* **14** 711
[24] Xu H, Liu H, Ling X, Sun Y and Yuan F 2017 *IEEE Trans. Antenn. Propag.* **65** 7378
[25] Wang J, Yang J, Fazal I M, Ahmed N, Yan Y, Huang H, Ren Y, Yue Y, Dolinar S, Tur M and Willner A E 2012 *Nat. Photon.* **6** 488
[26] Yan Y, Xie G, Lavery M P J, Huang H, Ahmed N, Bao C, Ren Y, Cao Y, Li L, Zhao Z, Molisch A F, Tur M, Padgett M J and Willner A E 2014 *Nat. Commun.* **5** 4876
[27] Yu N, Genevet P, Kats M A, Aieta F, Tetienne J P, Capasso F and Gaburro Z 2011 *Science* **334** 333
[28] Yang H, Cao X, Yang F, Gao J, Xu S, Li M, Chen X, Zhao Y, Zheng Y and Li S 2016 *Sci. Rep.* **6** 35692
[29] Xu B J, Wu C, Wei Z Y, Fan Y C and Li H Q 2017 *Opt. Mater. Express* **4** 1141
[30] Pu M, Li X, Ma X, Wang Y, Zhao Z, Wang C, Hu C, Gao P, Huang C, Ren H, Li X, Qin F, Yang J, Gu M, Hong M and Luo X 2015 *Sci. Adv.* **1** e1500396
[31] Xu B J, Wu C, Wei Z Y, Fan Y C and Li H Q 2016 *Opt. Mater. Express* **6** 3940
[32] Qi M Q, Tang W X and Cui T J 2015 *Sci. Rep.* **5** 11732
[33] Holloway C L, Kuester E F, Gordon J A, O'Hara J, Booth J and Smith D R 2012 *IEEE Antenn. Propag. Mag.* **54** 10
[34] Xiao S S 2017 *Research of electromagnetic beam controlling surface at KA frequency*, Master's Dissertation (Harbin: Harbin Institute of Technology) (in Chinese)
[35] Yan M Y, Sun Z C, Wu B R, Cheng P and Xu B J 2020 *Frontiers in Physics* **8** 46
[36] Sun Z C, Yan M Y, Mupona T E and Xu B J 2019 *Frontiers in Physics* **7** 181